DOE/NASA/10350-21
NASA TM-81594

Catalytic Combustion of Coal-Derived Liquids

Daniel L. Bulzan and Robert R. Tacina
National Aeronautics and Space Administration
Lewis Research Center

Work performed for
U.S. DEPARTMENT OF ENERGY
Fossil Energy
Office of Coal Utilization

Prepared for
Twenty-sixth Annual International Gas Turbine Conference
sponsored by the American Society of Mechanical Engineers
Houston, Texas, March 8-12, 1981

DOE/NASA/10350-21
NASA TM-81594

Catalytic Combustion of Coal-Derived Liquids

Daniel L. Bulzan and Robert R. Tacina
National Aeronautics and Space Administration
Lewis Research Center
Cleveland, Ohio 44135

Work performed for
U.S. DEPARTMENT OF ENERGY
Fossil Energy
Office of Coal Utilization
Washington, D.C. 20545
Under Interagency Agreement DE-AI01-77ET10350

Prepared for
Twenty-sixth Annual International Gas Turbine Conference
sponsored by the American Society of Mechanical Engineers
Houston, Texas, March 8-12, 1981

E-661

CATALYTIC COMBUSTION OF COAL-DERIVED LIQUIDS

Daniel L. Bulzan and Robert R. Tacina

National Aeronautics and Space Administration
Lewis Research Center
Cleveland, Ohio

ABSTRACT

A noble metal catalytic reactor was tested with three grades of SRC II coal-derived liquids, naphtha, middle distillate, and a blend of three parts middle distillate to one part heavy distillate. A petroleum-derived number 2 diesel fuel was also tested to provide a direct comparison. The catalytic reactor was tested at inlet temperatures from 600 to 800 K, reference velocities from 10 to 20 m/s, lean fuel-air ratios, and a pressure of $3x10^5$ Pa. Compared to the diesel, the naphtha gave slightly better combustion efficiency, the middle distillate was almost identical, and the middle-heavy blend was slightly poorer. The coal-derived liquid fuels contained from 0.58 to 0.95 % nitrogen by weight. Conversion of fuel nitrogen to NO_x was approximately 75 % for all three grades of the coal-derived liquids.

INTRODUCTION

An experimental study was conducted to demonstrate catalytic combustion of coal-derived liquids obtained from the SRC II process and also to determine some of the potential problems associated with fuel preparation and catalytic combustion of the fuels. Petroleum-derived diesel fuel was also tested to provide a direct comparison of reactor performance with the coal-derived fuels.

Lewis Research Center is currently evaluating catalytic combustion as part of the Critical Research and Advanced Technology Support Project sponsored by the DOE Office of Fossil Energy, Division of Coal Utilization. One of the objectives of this program is to develop combustor concepts for stationary gas turbines which will fire coal-derived liquid fuels in an environmentally acceptable manner. Coal-derived fuels typically contain high levels of nitrogen which are readily converted to NO_x during the combustion process. Coal-derived fuels have been tested in boilers (refs. 1 and 2) and gas turbine burners (ref. 3). Catalytic combustion of two coal-derived liquids, SRC II and H-Coal, is reported in reference 4. Catalytic combustion has demonstrated extremely low levels of thermal NO_x operation (refs. 5 and 6); however, it has also shown high conversions of fuel bound nitrogen to NO_x. Reference 4 reported essentially 100 % conversion of fuel bound nitrogen to NO_x for lean fuel-air ratios. Additional tests were needed to help determine if catalytic combustion offers potential benefits for the combustion of coal-derived liquids.

A noble metal catalytic reactor was tested at inlet temperatures up to 800 K, reference velocities from 10 to 20 m/s, and a pressure of $3x10^5$ Pa. Three grades of SRC II coal-derived liquids, naphtha, middle distillate, and a mid-heavy distillate blend, along with petroleum-based number 2 diesel fuel were tested. Performance and emissions of CO, CO_2, NO_x, and unburned hydrocarbons were measured.

EXPERIMENTAL DETAILS

Test Rig

The test rig is shown in Fig. 1. It was fabricated from 15.2-cm (6-in.-nominal-) diameter stainless steel pipe. Carborundum T30R fiberfrax tube insulation with a 12-cm inside diameter was inserted inside the pipe to minimize heat losses. A 0.16-cm thick stainless-steel liner was inserted inside the insulation upstream and downstream of the catalytic reactor to prevent erosion of the insulation.

The inlet air was indirectly preheated and temperatures were measured at a plane just upstream of the fuel injector with an array of 12 Chromel-Alumel thermocouples mounted in a flange. Test section inlet pressure was measured at a tap located in the flange containing the inlet thermocouples. Pressure was controlled by a back pressure valve. The airflow

entering the test rig was measured by a standard ASME orifice. Fuel flowrates were measured using linear mass flowmeters.

Two types of multiple point fuel injectors were used. The first was an airblast type while the second was an air-assist type. A module of the hexagonal tube airblast fuel injector is shown in Fig. 2(a). Nineteen modules were welded together to comprise the complete fuel injector. Fuel was injected through a 0.07-cm inside diameter tube pointing downstream in the center of the smallest cross-sectional area of each module to provide good atomization and mixing. All fuel tubes were the same length, 25.4 cm, to provide equal flowrates to each module. It was found the coal-derived liquids showed a tendency to plug the fuel tubes at elevated inlet air temperatures. As illustrated in Fig. 2(a), each fuel tube was surrounded by another tube to form a concentric tube arrangement. Air flowed through the 0.028-cm annulus to cool the fuel which prevented plugging of the fuel tubes. All testing was performed with cooling air flowing through the annulus. A module of the air-assist fuel injector is illustrated in Fig. 2(b). Fuel was injected downstream through the center, 0.024 cm inside diameter, tube. Air flowed through the outer ring of four, 0.051-cm inside diameter, tubes to assist in atomization and mixing of the fuel. It also provided cooling of the fuel tubes. Nineteen modules were used for the fuel injector. It was constructed such that the air-assist module arrangement was the same as the hexagonal tube module arrangement. The hexagonal tube modules, which made up the hexagonal tube fuel injector, were placed immediately upstream of the air-assist fuel injector to straighten the inlet velocity profile. A photograph of the air-assist fuel injector is shown in Fig. 3.

The premixing zone length of 30.6 cm was used for all fuels and fuel injectors. A single Chromel-Alumel thermocouple was used to detect any burning in the premixing zone. None was observed for these tests. The pressure drop across the fuel injector was measured with a differential pressure transducer connected between the inlet pressure tap and one located at the premixing region thermocouple station.

Two catalytic reactors were used for this study. The first was a uniform cell type while the second was a graded cell type. Both consisted of eight elements, 12 cm in diameter and 2.54 cm long, separated by a 0.31-cm gap containing at least one thermocouple. The last two elements were not separated. This arrangement is shown in Fig. 1. The reactor elements for both reactors are described in Table I. The pressure drop across the catalytic reactor was measured with a differential pressure transducer connected between a tap at the premixing zone thermocouple station and one located in the flange at the first row of thermocouples downstream of the catalytic reactor.

At a distance 17.2 cm downstream of the catalytic reactor, a single point water-cooled gas sampling probe, 0.6 cm inside diameter sampling passage, was used to withdraw samples for emissions measurements. Temperatures were also measured downstream of the reactor at the axial locations shown in Fig. 1. The gas sample line was electrically heated to keep unburned hydrocarbons from condensing. Concentrations of CO and CO_2 were measured with nondispersive infrared analyzers, unburned hydrocarbons with a flame ionization detector, and nitrogen oxides (total NO + NO_2) with a chemiluminescent analyzer.

MEASUREMENTS AND COMPUTATIONS

Reference Velocity

The reference velocity was computed from the measured mass flow rate, the average inlet air temperature, the duct cross-sectional area, and the test-section inlet pressure.

Emission Index

Emissions were measured as concentrations in ppm by volume, corrected for water of combustion, and converted to emission indices using the expressions in reference 7.

Combustion Efficiency

Combustion efficiency was calculated from the following expression:

$$EFF = 100 - 0.1\,(E.I._{HC} - E.I._{HC,EQ}) - 0.1\,\frac{HV_{CO}}{HV_{Fuel}}\,(E.I._{CO} - E.I._{CO,EQ})$$

where

EFF	combustion efficiency, %
$E.I._X$	emission index of specie X, g X/kg fuel
HV_X	lower heating value of X, J/kg

Equilibrium concentrations ($E.I._{X,EQ}$) were obtained from the computer program of reference 8.

Fuel-Air Ratio

The fuel-air ratio was determined both from the metered fuel flow and airflow rates and by making a carbon balance from the measured concentrations of CO, CO_2, and unburned hydrocarbons. The two values generally agreed within ±15 %. The adiabatic reaction temperature was computed from the computer program of reference 8 using the carbon balance fuel-air ratio. The carbon balance fuel-air ratio had the advantage that it was the local fuel-air ratio at which the emissions data were obtained. It also included the small amount of air (less than 3 % of the total airflow) used for cooling the fuel tubes.

RESULTS AND DISCUSSION

Three grades of SRC II coal-derived liquids and petroleum-derived number 2 diesel fuel were tested. The properties of the fuels are listed in Table II. As illustrated by the distillation curve values, the naphtha was the lightest grade tested and the mid-heavy blend (a blend of 2.9 to 1 of middle to heavy distillate) was the heaviest. Fuel nitrogen content of the coal-derived fuels ranged from 0.58 % for the naphtha to 0.95 % by weight for the mid-heavy blend. Hydrogen content varied from 12.09 % for the naphtha to 8.6 % by weight for the mid-heavy blend. Typical number 2 diesel fuel properties are listed for comparison. The testing sequence, along with the fuel injector and reactor used, is listed in Table III. All data presented were taken with the graded cell reactor of Table I(b) because problems developed with the uniform cell reactor, which will be discussed later.

Combustion Efficiency

Combustion efficiency for all fuels is presented in Fig. 4. Combustion efficiency at an inlet temper-

ature of 600 K is presented in Fig. 4(a). The naphtha gave the best efficiency. Run B and run C gave slightly poorer combustion efficiency than run A with diesel fuel. As shown in Table I.1, a different fuel injector was used for run B and run C than run A, because the air-assist fuel injector was damaged while being used for another program. The premixing zone was long enough so that the diesel fuel should have been essentially completely vaporized at the reactor inlet for both fuel injectors (ref. 9); therefore there should have been no effect of fuel injector type.

The difference could have been due to changes in catalyst activity, caused by testing the mid-heavy blend at an inlet temperature of 600 K. The first catalytic reactor element plugged when it was operated at an inlet temperature below 650 K. After the reactor plugged, the first and third catalytic elements were replaced with elements which were identical to the original elements. Any deposits which might have remained on the original elements could have caused the slight decline in combustion efficiency for run B and run C with diesel fuel, since both run B and run C were tested after the mid-heavy blend. Run B and run C with diesel fuel were identical in performance, indicating no loss of activity had occurred after approximately 8 hours of testing with the middle distillate fuel. The combustion efficiency of the middle distillate and the run B and run C with diesel fuel were almost identical.

Fig. 4(b) presents combustion efficiency at an inlet temperature of 700 K. The naphtha gave the best efficiency while the mid-heavy blend gave somewhat poorer efficiency than the other fuels. As previously discussed, a different fuel injector was used for the middle distillate fuel and the catalytic reactor could also have degraded slightly after being run on the mid-heavy blend. Therefore, the results of the diesel (run A) and the middle distillate can not be directly compared in this figure.

The effects of inlet temperature and reference velocity on combustion efficiency for middle-distillate fuel are presented in Figs. 5 and 6. An increase in the inlet temperature from 600 to 800 K resulted in a 50 K decrease in the adiabatic reaction temperature required for a combustion efficiency of 99.5 %. An increase in the reference velocity from 10 to 20 m/s at an inlet temperature of 800 K, required an adiabatic reaction temperature increase of 75 K to maintain a combustion efficiency of 99.5 %.

CO Emissions

The CO emission index for all fuels tested is presented in Fig. 7. Since most of the combustion inefficiency is due to CO emissions, they show the same trends as the combustion efficiency. The naphtha gave the lowest CO emissions and the mid-heavy blend gave the highest. At an inlet temperature of 600 K, CO emissions from the run B and run C with diesel fuel and the middle distillate were almost identical. Run A with diesel fuel gave slightly lower CO emissions than the other tests on diesel, run B and run C, probably caused by testing the mid-heavy blend at an inlet temperature of 600 K, as previously discussed.

The effect of inlet temperature and reference velocity on the CO emission index are presented in Figs. 8 and 9 for the middle distillate fuel. Again, the same trends as shown for combustion efficiency were found.

Unburned Hydrocarbons Emissions

The unburned hydrocarbons emission index for all fuels tested is presented in Fig. 10. The same trends with regard to fuel type as previously seen for CO emissions were found. The unburned hydrocarbons emission index for all three runs on diesel, run A, run B, and run C, was essentially identical. The slightly better combustion efficiency of run A with diesel fuel, seen previously, was due to lower CO emissions.

The effect of inlet temperature and reference velocity on the unburned hydrocarbons emission index are shown in Figs. 11 and 12. Little effect is evident.

NO_x Emissions

The NO_x (sum of NO + NO_2) emission index, expressed as g NO_2/kg fuel, for all the fuels tested at three inlet temperatures is presented in Fig. 13. As expected, NO_x emissions for the coal-derived liquids were considerably higher than the diesel fuel, due to the fuel bound nitrogen. The NO_x emission index for the mid-heavy blend was about 100 times the emission index for run A with diesel fuel.

NO_x emissions, expressed as ppm by volume and corrected to 15 % excess O_2, are shown in Figs. 14 and 15. Fig. 14 shows the effect of fuel, and Fig. 15 shows the effect of inlet temperature on NO_x emissions. The nitrogen oxides standard for new, modified, and reconstructed stationary gas turbines of 125 ppm at 15 % excess O_2 from reference 10 is shown for comparison. The 125 ppm standard includes an allowance of 50 ppm NO_x for fuels with a nitrogen content greater than 0.25 % by weight. The limit of 125 ppm is based on a gas turbine thermal efficiency of 25 % and is adjusted upward for increased thermal efficiencies. NO_x emissions for the coal-derived liquids ranged from a low of 41 ppm for the naphtha to a high of 304 ppm for the mid-heavy blend. They are also shown for the diesel fuel and were generally around 2 ppm. At an adiabatic reaction temperature necessary for a combustion efficiency of 99.5 % (from Fig. 4(a)), NO_x emission levels were 160 ppm for the naphtha, 250 ppm for the middle distillate, and 285 ppm for the mid-heavy blend, as given in Fig. 14(a). All are above the new source standard of 125 ppm. Fig. 15 illustrates an effect of reference velocity on NO_x emissions.

The conversion of fuel nitrogen in percent to NO_x is presented in Figs. 16, 17, and 18. Since thermal NO_x emissions are negligible at the relatively low temperatures of catalytic combustion (refs. 5 and 6), all measured NO_x was assumed to originate from fuel nitrogen. The solid symbols indicate combustion efficiencies greater than 99 %.

Fig. 16 presents the conversion in percent of fuel nitrogen to NO_x for the three coal-derived fuels at inlet temperatures of 700 and 800 K. For both inlet temperatures, conversion increased rapidly with adiabatic reaction temperature and then leveled off. The naphtha gave higher conversions to NO_x for a given adiabatic reaction temperature; however, combustion efficiency was also higher for the naphtha at that temperature.

The effect of inlet temperature on the conversion of fuel nitrogen to NO_x is presented in Fig. 17 for the middle distillate fuel. As previously seen, conversion increased rapidly with adiabatic reaction temperature and then leveled off. For a given adia-

batic reaction temperature, the higher inlet temperature gave a higher conversion; however, the data for all three inlet temperatures approached a maximum conversion of about 75 %.

Fig. 18 illustrates the effect of reference velocity (residence time) on the percent conversion of fuel nitrogen to NO_x at an inlet temperature of 800 K. Conversion approached 75 % at a reference velocity of 10 m/s, 60 % at 15 m/s, and about 55 % at 20 m/s. Since lower reference velocities gave an increased residence time in the catalytic reactor, increasing the catalytic bed residence time increases the conversion of fuel nitrogen to NO_x.

Pressure Drop

The pressure drop as a percentage of the inlet pressure is presented in Fig. 19 for middle distillate fuel at reference velocities of 10, 15, and 20 m/s. At an adiabatic reaction temperature of 1350 K, the pressure drop ranged from 1.6 % at 10 m/s to 3.6 % at 20 m/s. This is reasonable for an application.

Other Results

Photographs of the fuel injector and the catalytic reactor (graded cell reactor of Table I(b)) after testing the mid-heavy blend are presented in Fig. 20. Figs. 20(a) and (b) show the reactor and fuel injector after operating on the mid-heavy blend at inlet temperatures of 650 K. A deposit of about 0.32 cm thickness was formed on the front edges of the first reactor element. The fuel injector also had deposits which were formed on each fuel injector module. Fig. 20(c) shows a portion of the first reactor element after it was operated at an inlet temperature of 600 K. As previously discussed, the front element quickly plugged at the lower inlet temperature which probably was caused by the decreased vaporization of the mid-heavy blend at 600 K.

A photograph of the uniform cell reactor, described in Table I(a), is presented in Fig. 21 after it was operated at an inlet temperature of 600 K on the naphtha grade fuel. The reactor quickly plugged after the naphtha fuel was introduced. No further tests were made using the uniform cell reactor. Reference 11 reported decreased wall temperatures for the front elements of a uniform cell reactor as opposed to a graded cell type. It was found that the first element required a considerably longer length to increase from the inlet temperature to the adiabatic reaction temperature for the uniform cell reactor. This is probably the cause for the plugging of the uniform cell reactor on the naphtha fuel while the graded cell reactor operated on the fuel without any problems.

SUMMARY OF RESULTS

This study has demonstrated catalytic combustion of three grades of coal-derived liquids obtained from the SCR II process. The three grades tested were a naphtha, a middle distillate, and a mid-heavy distillate blend. Petroleum-derived diesel fuel was also tested to provide a direct comparison of catalytic reactor performance with the coal-derived fuel. Compared to the diesel, the naphtha was better than the diesel in combustion efficiency, the middle distillate was approximately equal to, and the mid-heavy blend was poorer than the diesel. The mid-heavy blend required inlet temperatures of at least 650 K to prevent plugging the channels of the first catalytic element.

The coal-derived fuels contained from 0.58 to 0.95 % of nitrogen by weight. Under the fuel lean conditions tested, catalytic combustion, which is capable of producing negligible thermal NO_x emissions, was an efficient converter of fuel bound nitrogen to NO_x. Conversion levels ranged as high as 75 %. The emission standard of 125 ppm NO_x at 15 % excess O_2 could not be met with any of the coal-derived fuels tested.

The catalytic reactor was operated for about 16 hours on the synthetic fuels. While no significant loss of activity or poisoning of the catalyst was apparent for the conditions tested, the application of catalytic combustion to stationary gas turbines would require operation for thousands of hours.

REFERENCES

1. Hersch, S., et al., "Combustion Demonstration of SRC II Fuel oil in a Utility Boiler," ASME Paper 79-WA/FU-7, Dec. 1979.
2. Downs, W., et al., "Characterization and Combustion of SRC II Fuel Oil," ASME Paper 79-WA/FU-2, Dec. 1979.
3. Pillsbury, P. W., et al., "Fuel Effects in Recent Combustion Turbine Burner Tests of Six Coal Liquids," ASME Paper 79-FT-137, Mar. 1979.
4. Chu, E. K., G. C. Snow, and H. Tong, "Catalyst Combustion of Coal-Derived Liquid Fuels," Report 80-45/EE, Acurex Corp., Mountain View, Calif., 1980.
5. Anderson, D. N., "Performance and Emissions of a Catalytic Reactor with Propane, Diesel, and Jet A Fuels," NASA TM-73786, 1977.
6. Pfefferle, W. C., et al., "CATATHERMAL Combustion: A New Process for Low-Emissions Fuel Conversion," ASME Paper 75-WA/FU-1, Dec. 1975.
7. "Procedure for the Continuous Sampling and Measurement of Gaseous Emissions from Aircraft Turbine Engines," Aerospace Recommended Practice 1256, SAE, Oct. 1, 1971.
8. Gordon, S. and B. J. McBride, "Computer Program for Calculation of Complex Chemical Equilibrium Compositions, Rocket Performance, Incident and Reflected Shocks, and Chapman - Jouguet Detonations," NASA SP-273, Rev. 1976.
9. Tacina, R. R., "Degree of Vaporization Using an Airblast Type Injector for a Premixed-Prevaporized Combustor," NASA TM-78836, 1978.
10. "Environmental Protection Agency, Standards of Performance for New Stationary Sources; Gas Turbines," Federal Register, Vol. 44, No. 176, Part II, Sept. 10, 1979, pp. 52792-52798.
11. Kesselring, J. T., W. V. Krill, S. J. Anderson, and H. L. Atkins, "Recent Advances in Catalytic Combustion System Development," ASME Paper 79-WA/FU-8, Dec. 1979.

TABLE I. - DESCRIPTION OF CATALYTIC REACTOR ELEMENTS

(a) Uniform cell reactor

Element	Catalyst material	Catalyst loading, kg/m^3	Substrate manufacturer	Substrate material	Cell density, $cells/cm^2$	Open area, %
1	Pt	3.6	Gen. Refactories	Cordierite	34	67
2	↓	↓	↓	↓	↓	↓
3						
4						
5	1 Pt/2 Pd		Corning		46.5	63
6						
7						
8	↓	↓	↓	↓	↓	↓

(b) Graded cell reactor

Element	Catalyst aterial	Catalyst loading, kg/m^3	Substrate manufacturer	Substrate material	Cell density, $cells/cm^2$	Open area, %
1	Pt/Pd	3.6	Dupont	Mullite	2.6	75
2	Pt/Pd		↓	↓	2.6	75
3	Pd				9.3	60
4	Pd				9.3	60
5	2 Pd/1 Pt		Corning	Cordierite	46.5	63
6						
7						
8	↓	↓	↓	↓	↓	↓

TABLE II. - DESCRIPTION OF FUELS

	Naphtha	Middle distillate	Mid-heavy blend	Diesel
Distillation, K				
IBP	336	448	443	456
10	356	480	484	497
20	373	490	495	509
50	408	512	522	537
70	431	528	546	556
90	466	549	627	583
FBP	487	578	644	606
Elementals, % by weight				
Carbon	84.62	85.59	86.21	86.7
Hydrogen	12.09	9.06	8.64	13.0
Nitrogen	.58	.87	.95	.014
Sulfur	.38	.29	.21	.28
Oxygen (by difference)	2.33	4.19	3.99	------
Specific gravity (289 K)	0.832	0.982	0.999	0.847
Viscosity, cS	0.816 @ 311 K	6.02 @ 296 K	4.527 @ 311 K	3.8 @ 296 K
Gross heat of combustion, J/kg	4.220×10^7	4.020×10^7	3.996×10^7	4.453×10^7
Volume % aromatics	17.1	---	84.3	39.27

TABLE III. - RUN SEQUENCE

Sequence	Fuel	Fuel injector	Reactor
1	Naphtha	Air-assist	Uniform cell
2	Diesel (Run A)	↓	Graded cell
3	Naphtha		↓
4	Mid-heavy blend		
5	Diesel (Run B)	Hexagonal tube	
6	Middle-distillate	↓	
7	Diesel (Run C)		

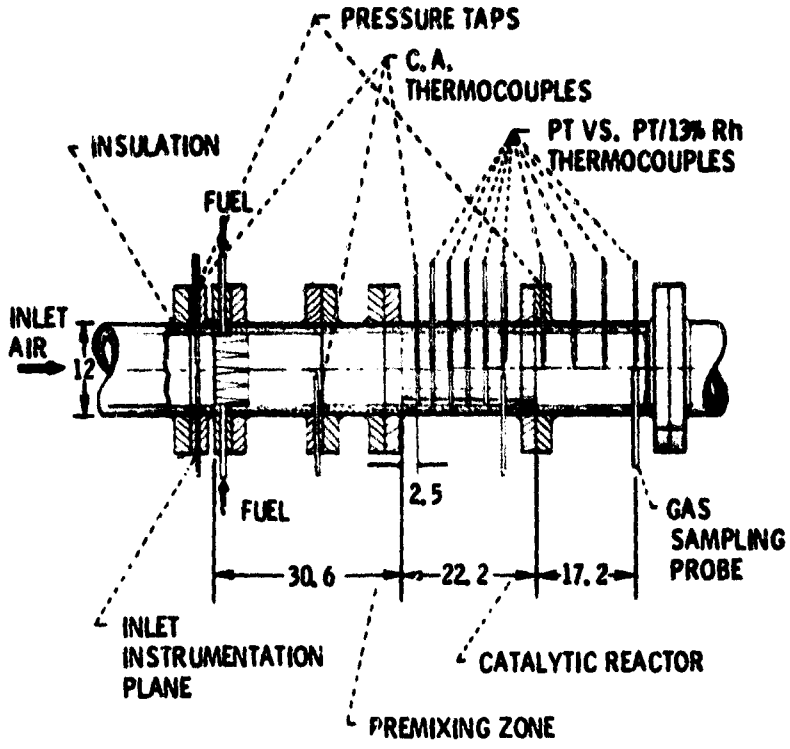

Figure 1. - Test section, hexagonal tube fuel injector shown. (Dimensions in cm.)

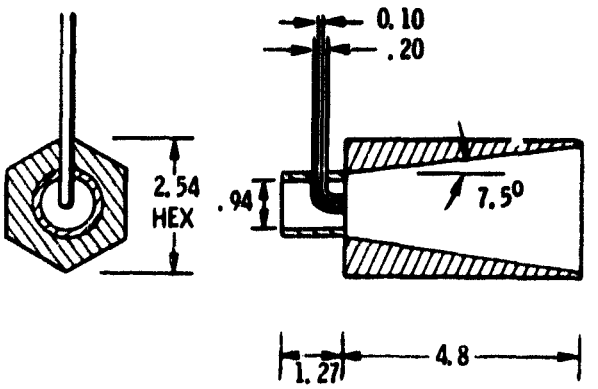

(a) HEXAGONAL TUBE MODULE (ONE OF 19).

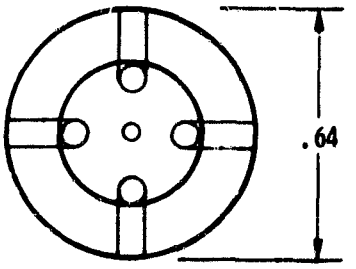

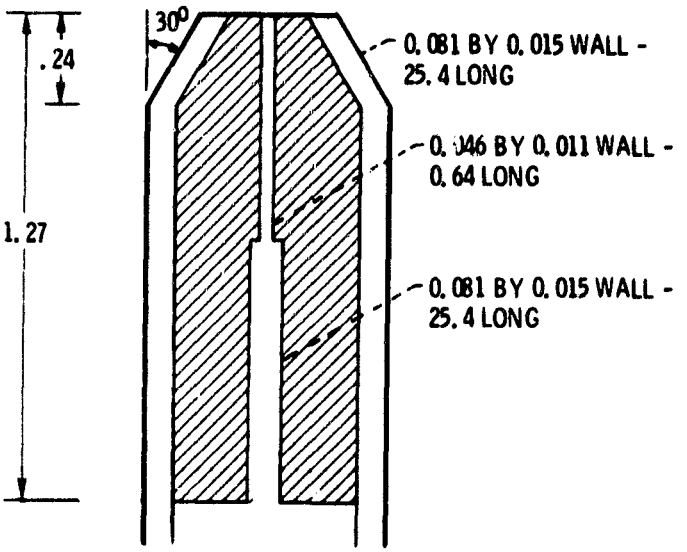

(b) AIR-ASSIST MODULE (ONE OF 19).

Figure 2. - Fuel injector module. (Dimensions in cm.)

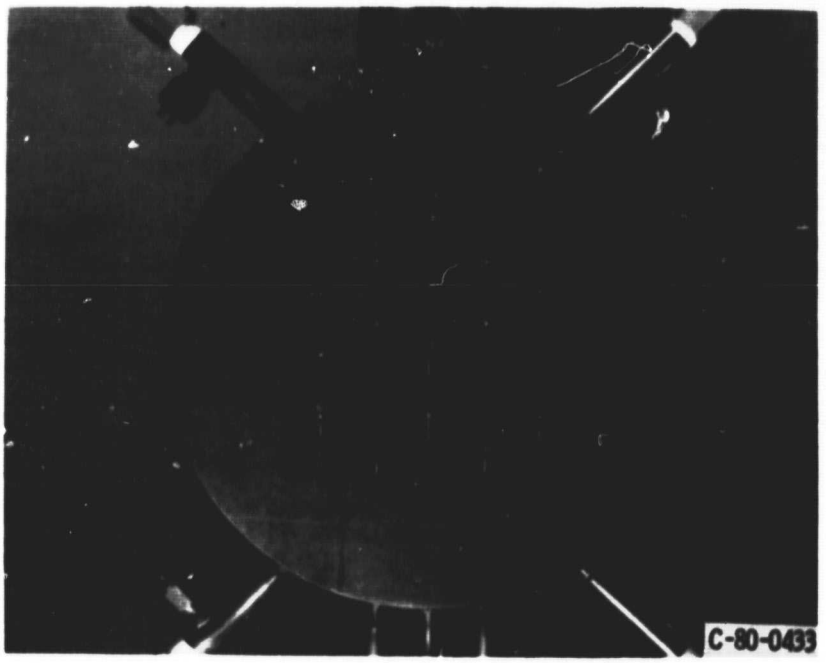

Figure 3. - Air-assist fuel injector.

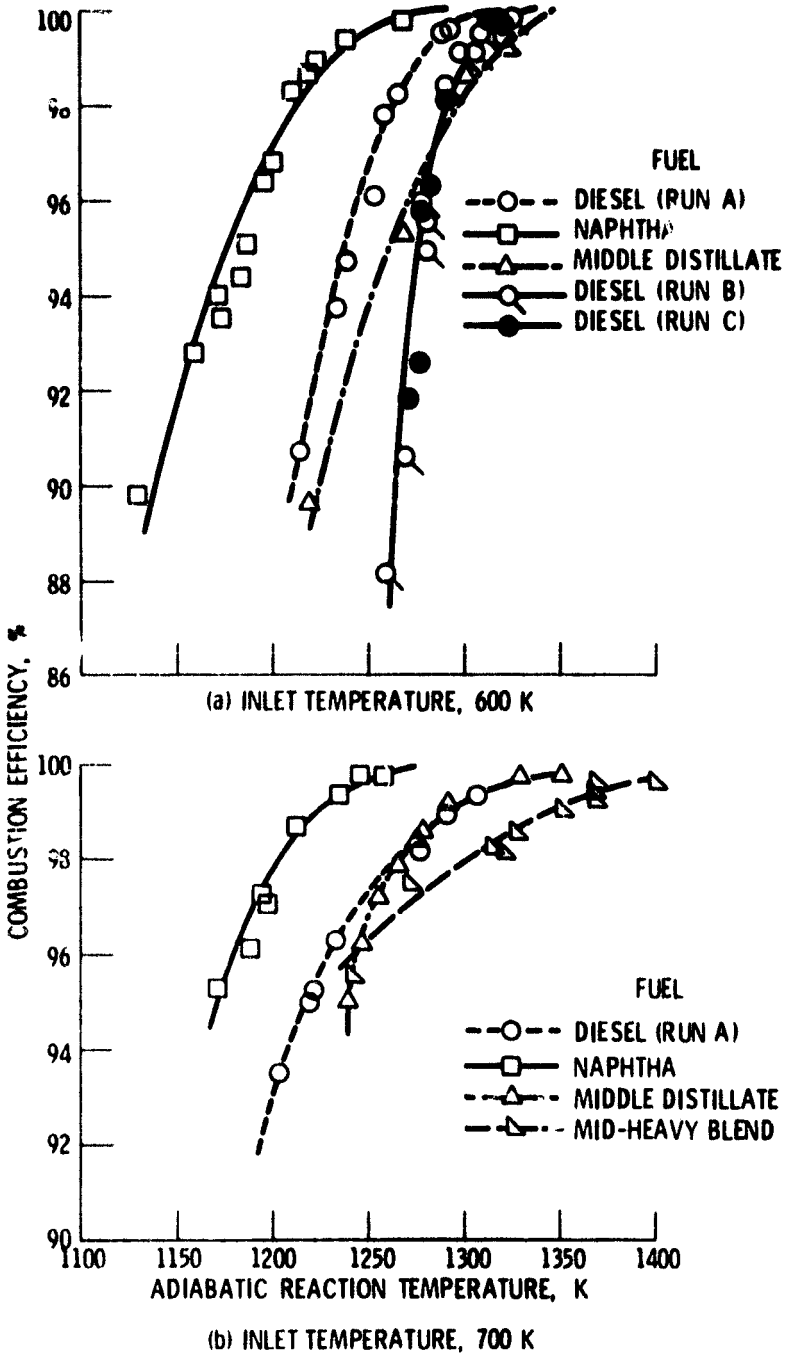

Figure 4. - Effect of fuel type on combustion efficiency. Reference velocity, 10 m/s; pressure, 3×10^5 Pa.

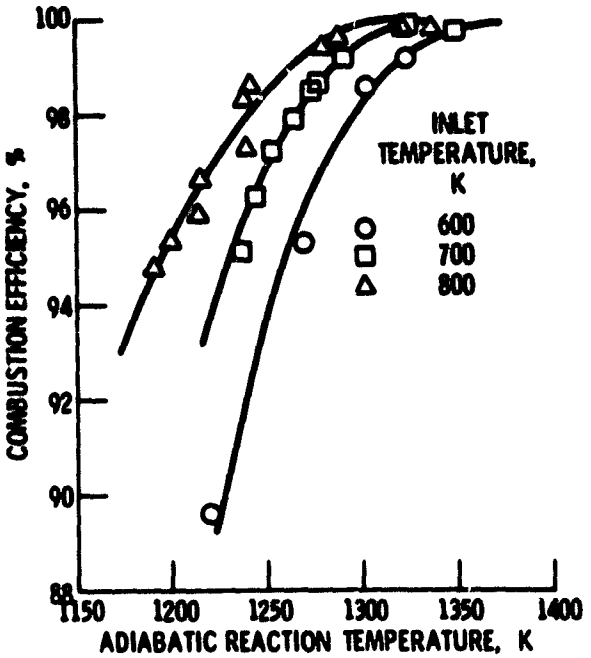

Figure 5. - Effect of inlet temperature on combustion efficiency. Middle distillate fuel; reference velocity, 10 m/s; pressure, 3×10^5 Pa.

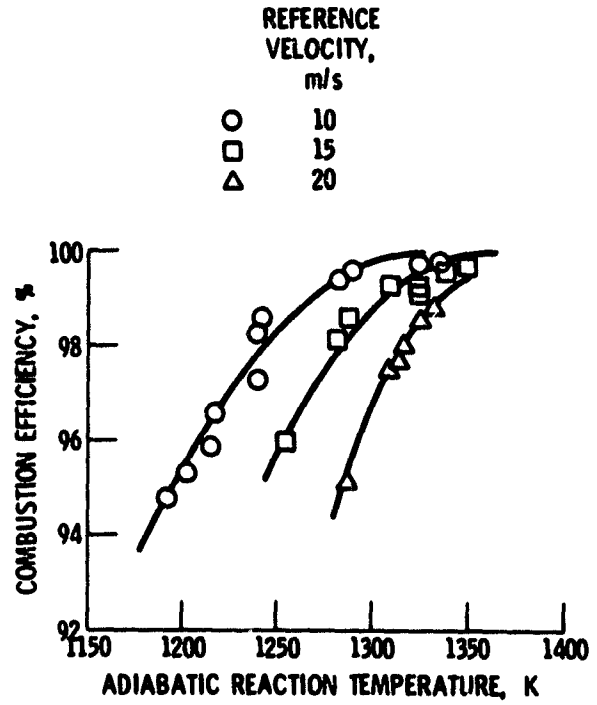

Figure 6. - Effect of reference velocity on combustion efficiency. Middle distillate fuel; inlet temperature 800 K; pressure, 3×10^5 Pa.

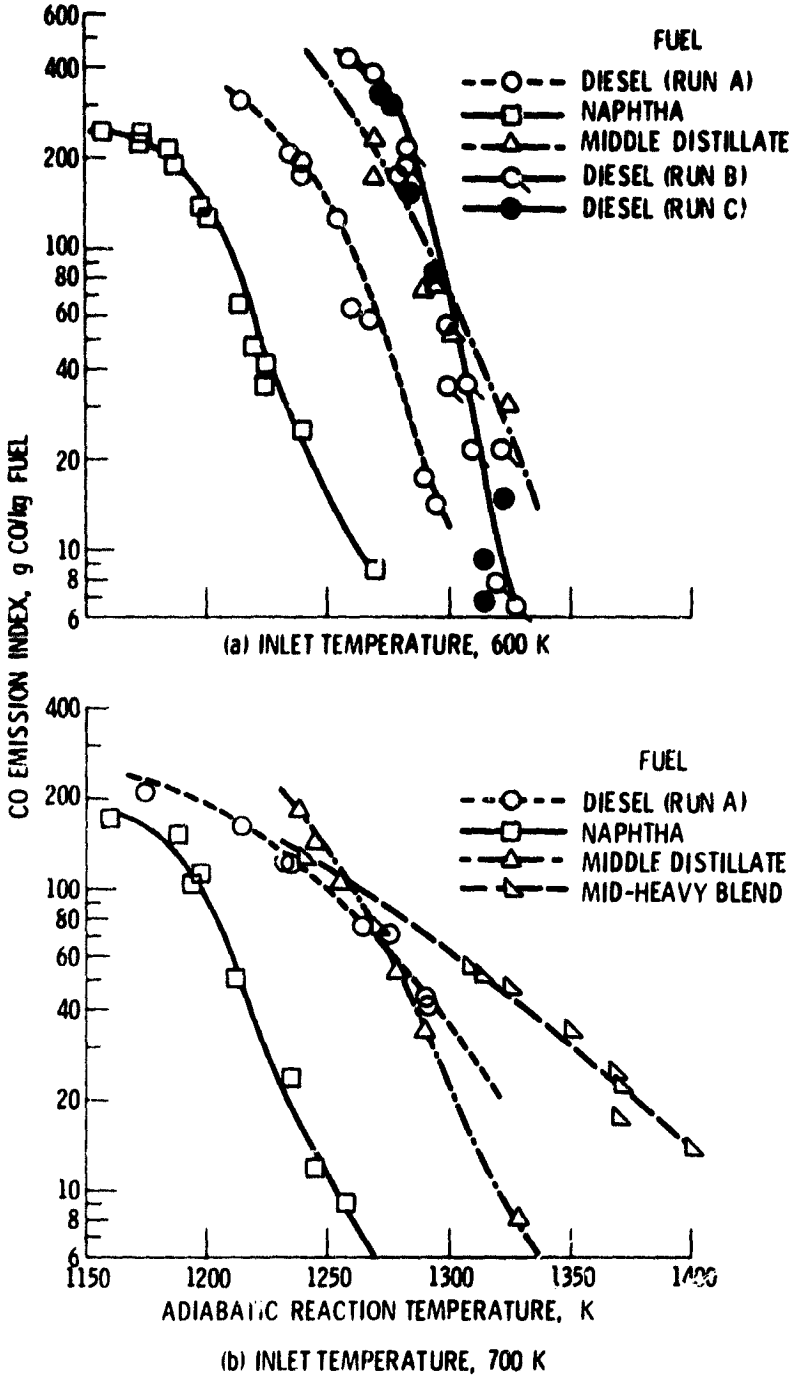

Figure 7. - Effect of fuel type on CO emission index. Reference velocity, 10 m/s; pressure, 3×10^2 Pa.

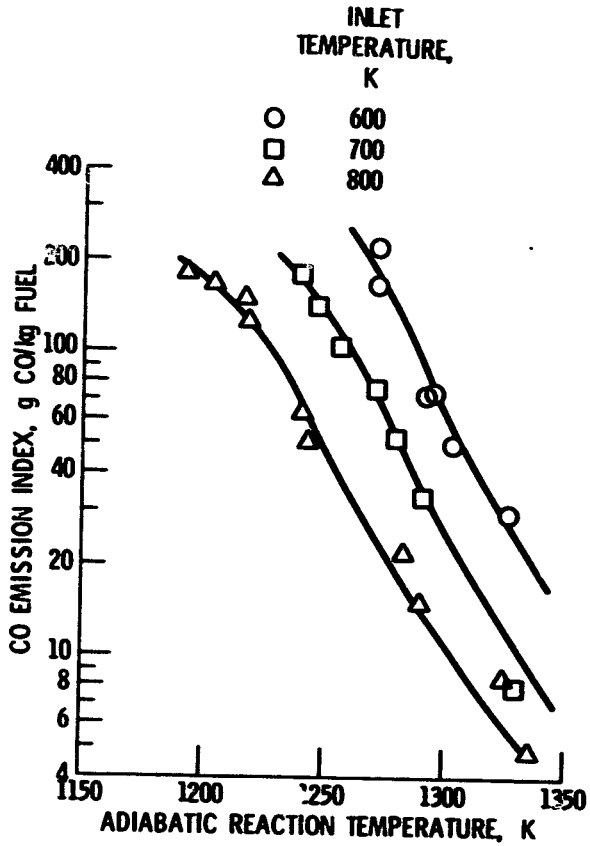

Figure 8. - Effect of inlet temperature on CO emission index. Middle distillate fuel; reference velocity, 10 m/s; pressure, 3×10^5 Pa.

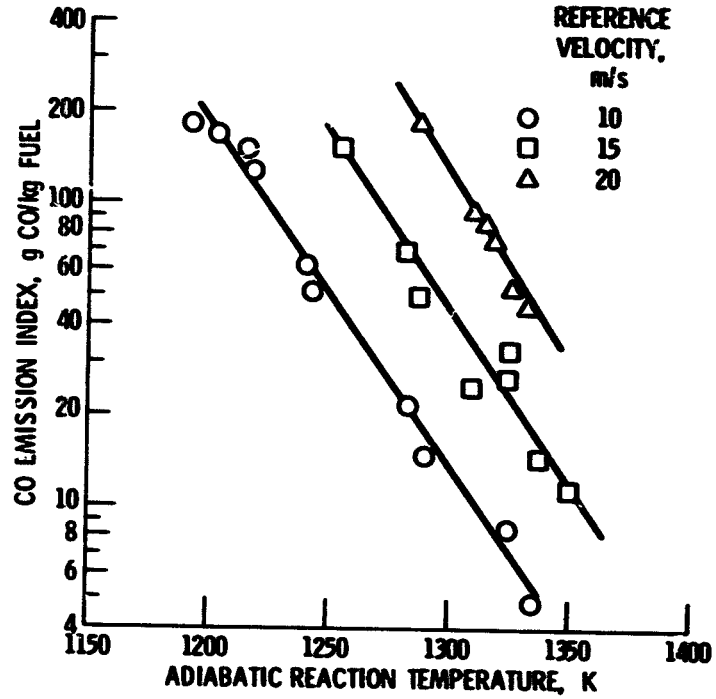

Figure 9. - Effect of reference velocity on CO emission index. Middle distillate fuel; inlet temperature, 800 K; pressure, 3×10^5 Pa.

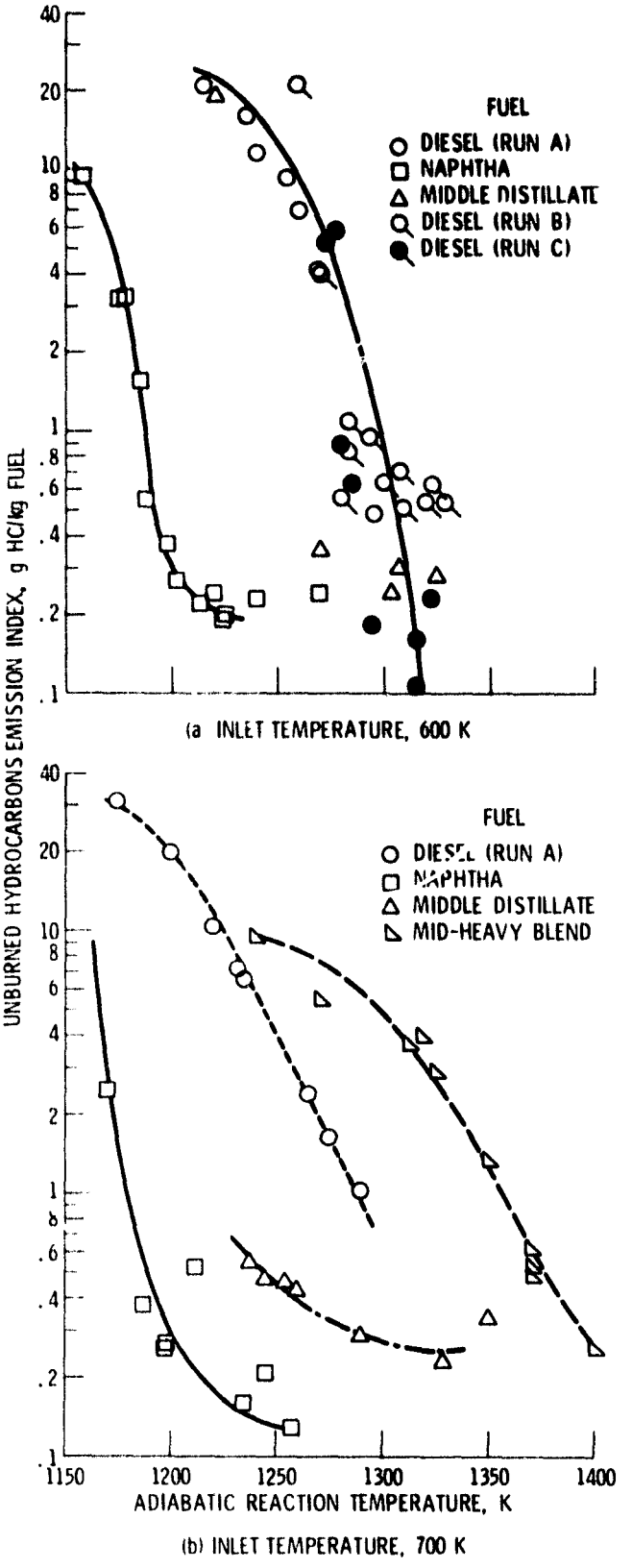

Figure 10. - Effect of fuel type on unburned hydrocarbons emission index. Reference velocity, 10 m/s; pressure, 3×10^5 Pa.

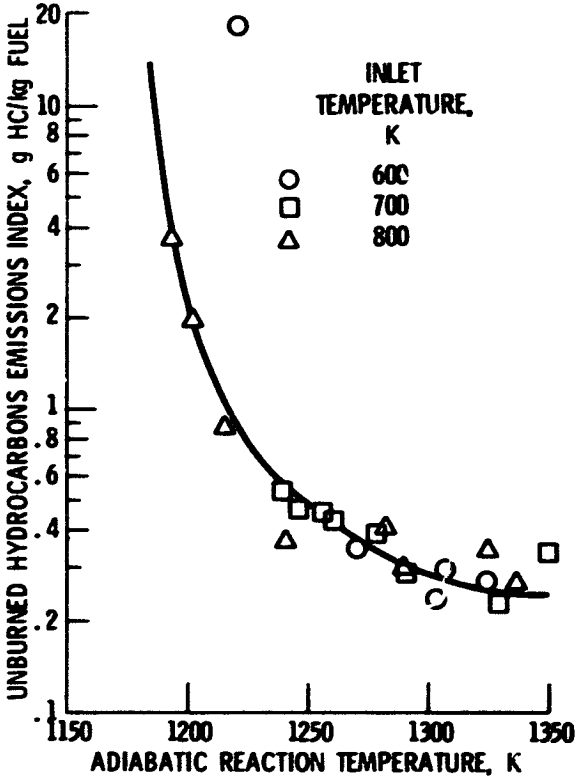

Figure 11. - Effect of inlet temperature on unburned hydrocarbons emission index. Middle distillate fuel, reference velocity, 10 m/s; pressure, 3×10^5 Pa.

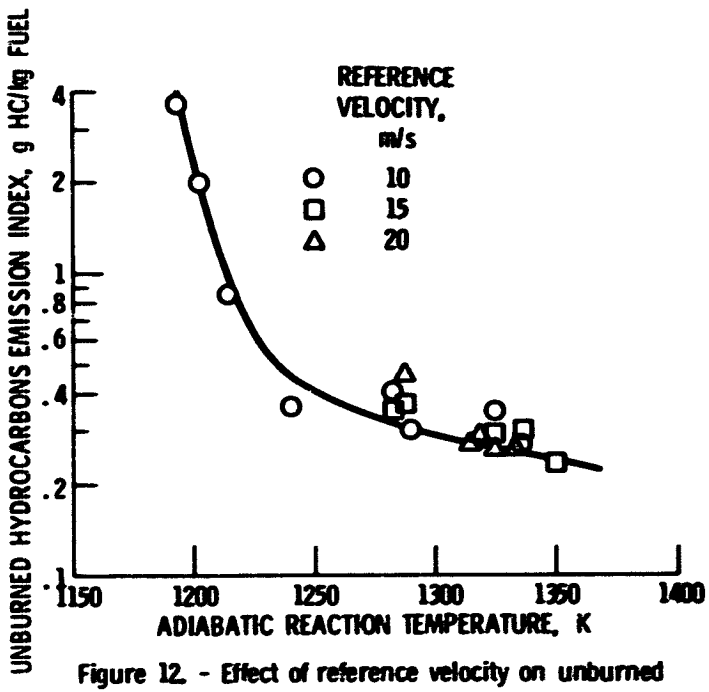

Figure 12. - Effect of reference velocity on unburned hydrocarbons emission index. Middle distillate fuel; inlet temperature, 800 K; pressure, 3×10^5 Pa.

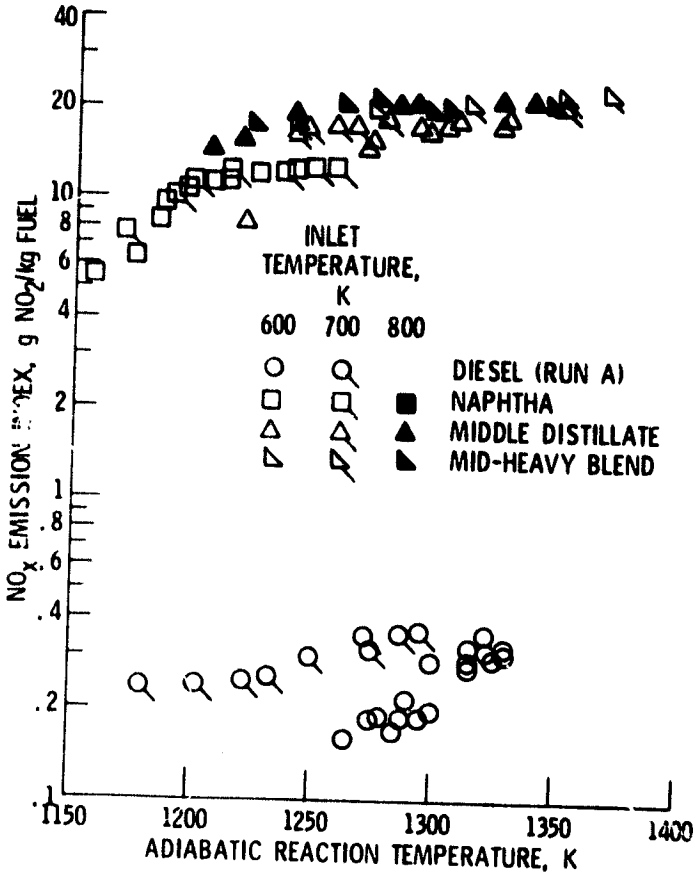

Figure 13. - NO_x emission index; reference velocity, 10 m/s; pressure, 3×10^5 Pa.

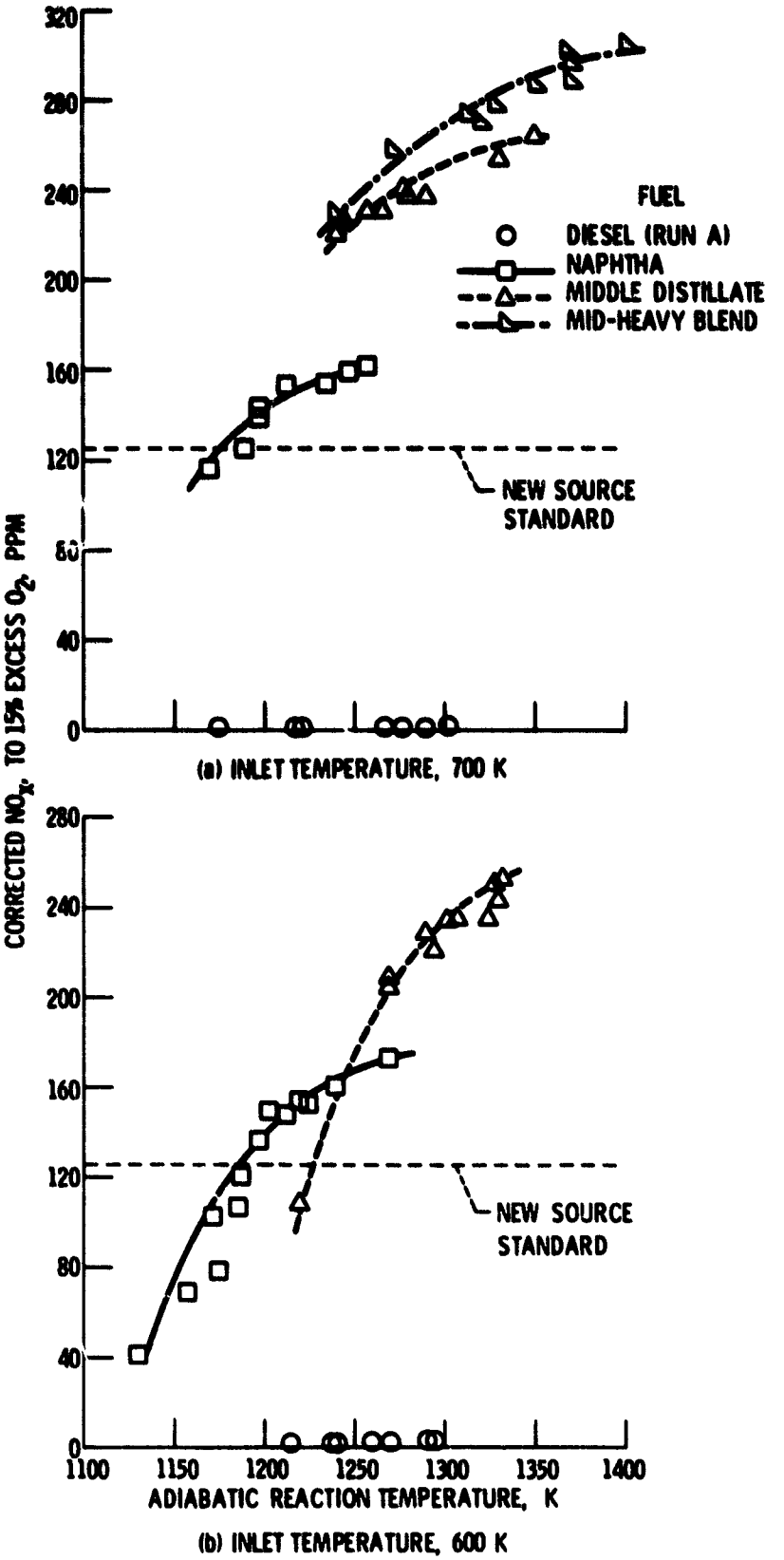

Figure 14. - Effect of fuel type on NO_x emissions. Reference velocity, 10 m/s; pressure, 3×10^5 Pa.

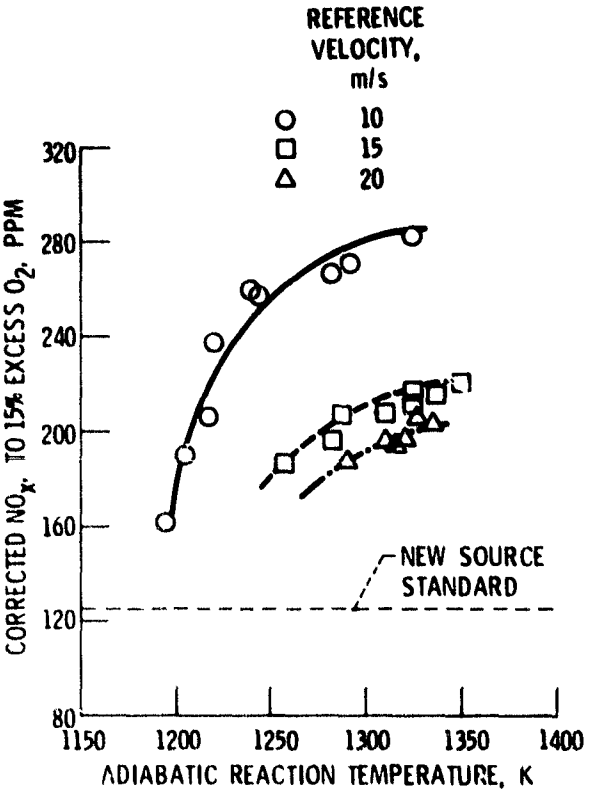

Figure 15. - Effect of reference velocity on NO_x emissions. Middle distillate fuel; inlet temperature, 800 K; pressure, 3×10^5 Pa.

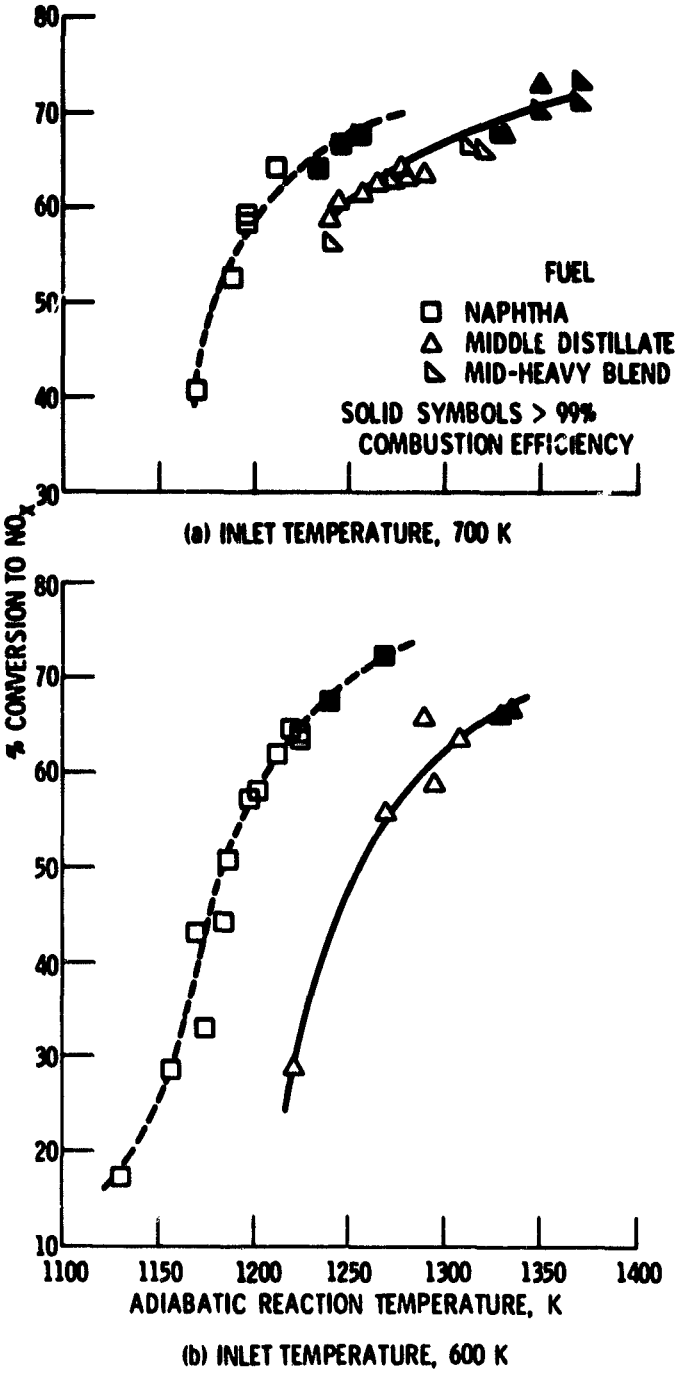

Figure 16. - Effect of fuel on conversion of fuel nitrogen to NO_x. Reference velocity, 10 m/s; pressure, 3×10^5 Pa.

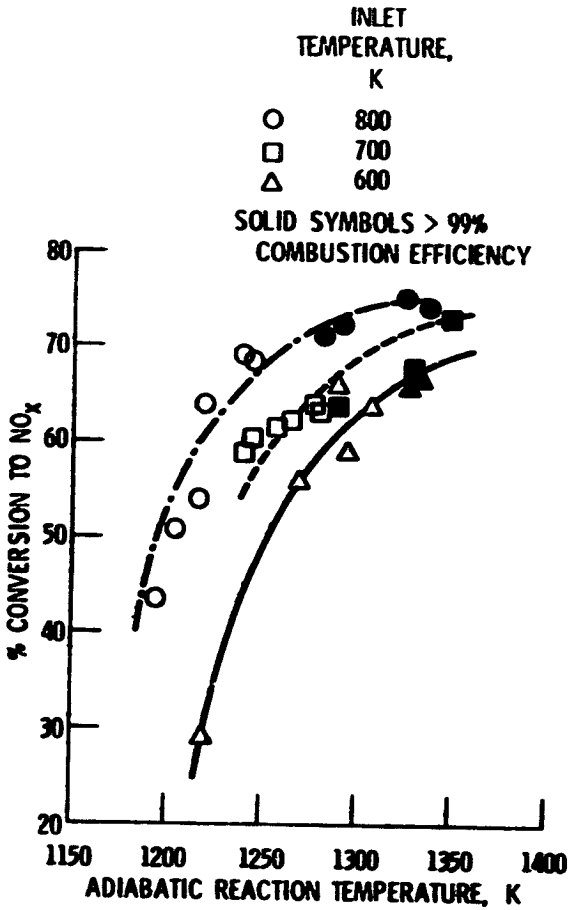

Figure 17. - Effect of inlet temperature on fuel nitrogen conversion to NO_x. Middle distillate fuel; reference velocity, 10 m/s; pressure, 3×10^5 Pa.

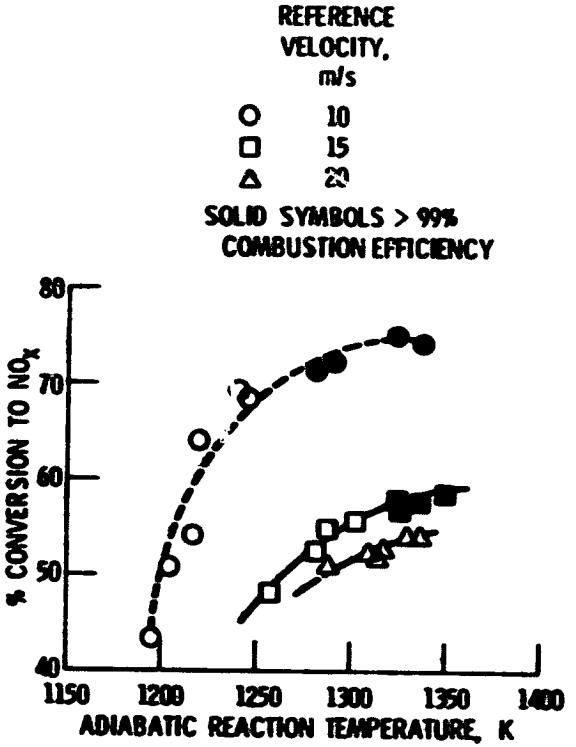

Figure 18. - Effect of reference velocity on fuel nitrogen conversion to NO_x. Middle distillate fuel; inlet temperature, 800 K; pressure, 3×10^5 Pa.

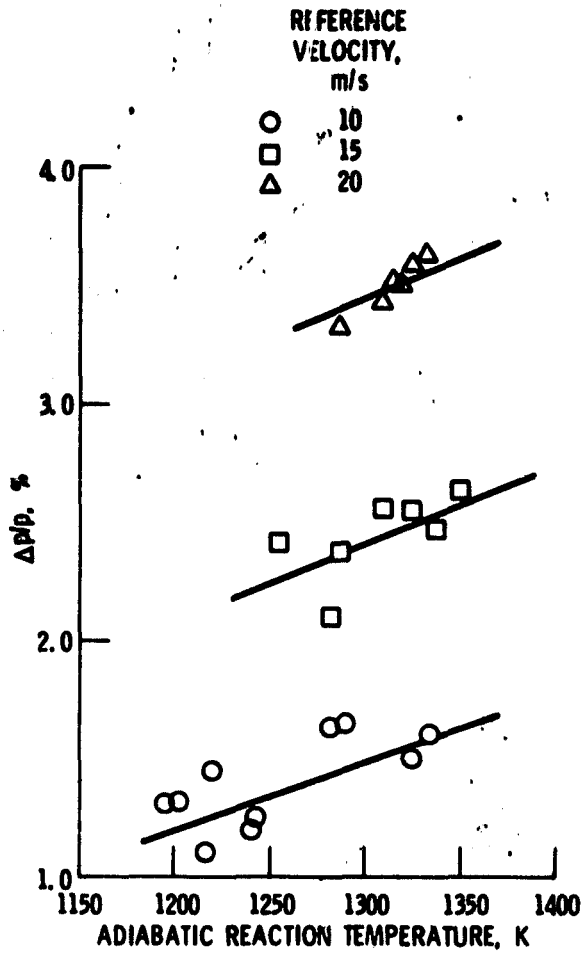

Figure 19. - Effect of reference velocity on pressure drop. Middle distillate fuel; inlet temperature, 800 K; pressure 3×10^5 Pa.

(a) REACTOR

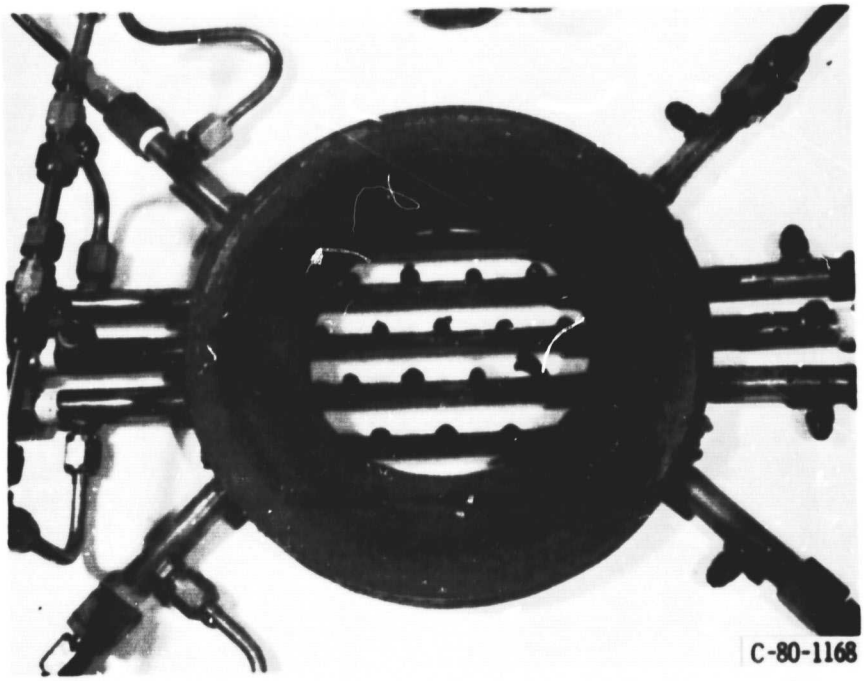

(b) AIR-ASSIST FUEL INJECTOR

Figure 20. - Fuel injector and reactor after mid-heavy blend tests.

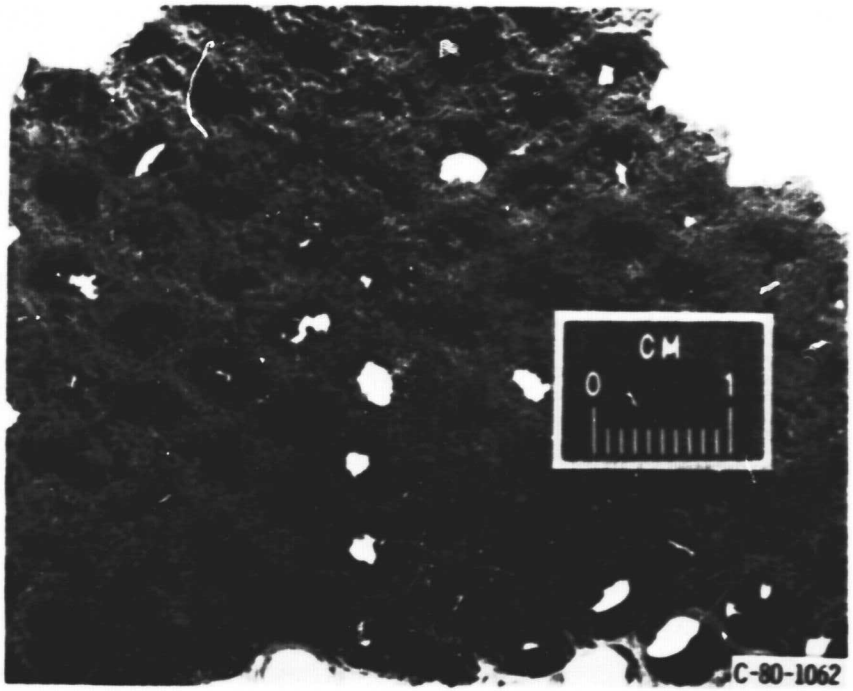

(c) AFTER 600K INLET OPERATION, PORTION OF 1st ELEMENT.

Figure 20. - Conciuded.

Figure 21. - Uniform cell reactor, after naphtha at 600K inlet.